Characterization of Polyisoprene-*b*-Poly(methyl methacrylate) Diblock Copolymer Micelles in Acetonitrile[||]

Karin Schillén,[†] Ahmad Yekta,[‡] Shaoru Ni, J. P. S. Farinha,[§] and Mitchell A. Winnik*

Department of Chemistry, University of Toronto, 80 St. George Street, Toronto, Ontario, Canada M5S 3H6

Received: January 22, 1999

In acetonitrile, polyisoprene-*b*-poly(methyl methacrylate) (PI−PMMA) diblock copolymers form starlike micelles with a dense core of the insoluble PI blocks and a soft solvent-swollen corona of the soluble PMMA blocks. Static and dynamic light scattering experiments in combination with viscosity measurements show that these micelles behave hydrodynamically as hard spheres. The block copolymers are labeled at the block junction, with a single fluorescent dye, either a donor chromophore (phenanthrene) or an acceptor chromophore (anthracene). These dyes are confined to the interface during self-assembly. Fluorescence energy-transfer experiments on molecularly mixed micelles of donor- and acceptor-labeled copolymers provide a core radius of 7.6 ± 0.8 nm and a number-average aggregation number (N_n^{agg}) of 98 ± 22 under the assumption that the energy transfer takes place on a surface of a sphere. Simulations in terms of a Helfand−Tagami junction distribution profile confirm that the core−corona interface of the PI−PMMA micelles is thin (ca. 0.9 nm) and that almost all of the energy transfer occurs within a narrow interfacial region. From the static light scattering measurements of the mixed micelles a weight-average aggregation number (N_w^{agg}) of 127 ± 6 is obtained. The ratio $N_w^{agg}/N_n^{agg} = 1.3$ agrees with size polydispersity of the micelles obtained from the analysis of dynamic light scattering data. The experimental corona thicknesses are in good agreement with those calculated from expressions describing starlike block copolymer micelles.

Introduction

A diblock copolymer is a polymer which consists of two sequences of monomer units of different chemical composition attached at a common junction. When these polymers are dissolved in a medium which is a good solvent for one of the blocks and a nonsolvent for the other, the polymers associate to form micelles. Each micelle consists of a core of the insoluble blocks surrounded by a solvent-swollen corona of the soluble block. The core may be compact or swollen by the solvent, depending on the extent of miscibility of the solvent with the core polymer. Micelle formation by di- and triblock copolymers in both organic solvents and in water have been investigated by a variety of different experimental methods, including scattering techniques (light, small-angle X-ray (SAXS) and small-angle neutron (SANS) scattering), fluorescence spectroscopy, and electron microscopy. The individual blocks of the copolymers may be nonionic or ionic, which leads to a broad variation in solution behavior. [1,2] Depending on the relative size of the blocks, the quality of the solvent, and the method of micelle preparation, one can obtain micelles with different shapes. For example, spherical,[3] rodlike[4−6] or wormlike[7] aggregates have been identified. For these micelles, the core is often considered to be liquidlike when studied at temperatures above the glass transition temperature (T_g) of the core polymer component. Several good reviews of block copolymer micelles have been published.[8−11]

The aggregation number of block copolymer micelles is normally determined by static light scattering experiments, and the hydrodynamic radius (R_H) is measured by dynamic light scattering. Features of the internal structure, such as the core radius (R_{core}) and the corona thickness (L) of various block copolymer micelles have been investigated by SANS or SAXS measurements, often in combination with light scattering experiments.[12−16] Many of these results have been compared successfully to the predictions of the starlike model or the brushlike (crew-cut) model of a polymeric micelle.[16−19]

The theory of block copolymer micelles treats polymer micelles at equilibrium. For micelles to reach equilibrium, the micelles must be in a state of dynamic exchange with individual polymer molecules ("unimers") in solution. In many examples, the micelles are not in dynamic equilibrium under the conditions in which the measurements were made. These micelles are dynamically "frozen." No significant exchange of unimers among micelles takes place, either because the micelle core is glassy or crystalline or because the solubility of the core-forming block in the solvent is so low (i.e., the Flory−Huggins interaction parameter between the core-forming block and the solvent is too large). In some systems, with slow exchange of solvent or change in temperature, the micelles pass through a stage of dynamic equilibrium during their preparation. In other systems, the history of preparation will influence the micellar size.[1,20,21]

[||] We dedicate this paper to the 65th birthday of Professor J. K. Thomas in honor of his many accomplishments over his long career.

* To whom correspondence should be addressed. E-mail: mwinnik@chem.utoronto.ca.

[†] Present address: Physical Chemistry 1, Center for Chemistry and Chemical Engineering, Lund University, P. O. Box 124, S-221 00 Lund, Sweden. E-mail address: Karin.Schillen@fkem1.lu.se.

[‡] Present address: Imaging Research Inc., 500 Glenridge Ave., St. Catherines, Ontario, L2S-3A1, Canada.

[§] On leave from: Centro de Química-Física Molecular, Complexo I, Instituto Superior Técnico, Av. Rovisco Pais, 1096 Lisboa Codex, Portugal. E-mail: farinha@chem.utoronto.ca.

10.1021/jp990251y CCC: $18.00 © 1999 American Chemical Society
Published on Web 05/06/1999

CHART 1

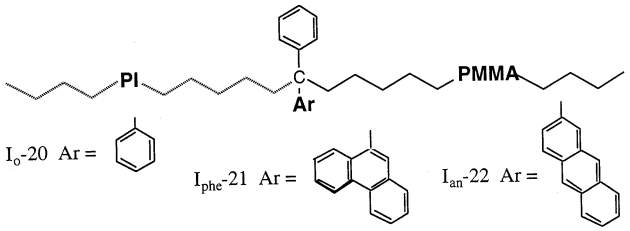

In this paper, we report studies of micelle formation by three samples of polyisoprene-*b*-poly(methyl methacrylate), PI−PMMA, in acetonitrile (CH_3CN). The block copolymers are shown in Chart 1. In each of these samples, the PI has a degree of polymerization of approximately 150, whereas the PMMA block is significantly longer (ca. 500 monomers). One polymer, I_0-24, is "unlabeled": the two phenyl rings at the PI/PMMA junction derive from the use of 1,1-diphenyl ethylene to terminate the living anion of PI prior to addition of MMA in the synthesis of the polymer. Analogous methods were used to introduce the 9-phenanthryl group into I_{phe}-21 and the 2-anthryl chromophore into I_{an}-22. These polymers form spherical starlike micelles in acetonitrile, which we characterize by a combination of viscosity and light scattering techniques. An interesting feature of these experiments is that acetonitrile is actually a poor solvent for the PMMA corona chains. Our experiments are carried out at a temperature nearly 20 °C below the Θ temperature for PMMA in CH_3CN. Nevertheless, the micelle behave hydrodynamically as hard spheres and exhibit a small but positive second virial coefficient in the light scattering experiments.

In addition, we show that direct nonradiative energy transfer (DET) measurements[22,23] on mixed micelles containing both I_{phe}-21 and I_{an}-22 allow one to determine both the core radius and the number-averaged aggregation number (N_n^{agg}) of the micelles. The analysis of the fluorescence decay data takes advantage of recent advances in the theory of energy transfer in restricted geometries.[24−27] This number is somewhat smaller than the weight-averaged value (N_w^{agg}) determined by static light scattering. The micelle polydispersity determined in this way is close to that calculated from a cumulant analysis of the dynamic light scattering data. Some aspects of the energy-transfer experiments were published previously.[28,29]

DET measurements on junction-labeled PS−PMMA diblock copolymers have been used to examine the core-corona interface of their micelles in dioxane−methanol.[30] Here the extent of data analysis was limited due to the extensive swelling of the micelle core by the solvent. Other applications of energy transfer have been to monitor the rate of unimer exchange and to investigate micellar dissociation for block copolymer micelles in selective solvents.[31−35] Recently, the increase in energy-transfer efficiency was employed to follow micelle formation of fluorene- and pyrene-labeled polystyrene-*b*-poly(2-hydroxyethyl methacrylate) copolymers in tetrahydrofuran/cyclohexane mixtures.[36] Liu has proposed energy-transfer experiments different from those reported here for determining the core radius of block copolymer micelles.[36,37] Excimer fluorescence has also been used for detection of micelle formation, for example, of naphthalene-labeled graft copolymers of polystyrene-*alt*-maleic anhydride-*graft*-poly(ethylene oxide) in dioxane/water mixtures.[38] For other references on the use of energy-transfer measurements to characterize polymer surfaces and interfaces, the reader is referred to previous publications from our group[24,39] and references cited therein.

TABLE 1: Characteristics of the PI−PMMA Diblock Copolymers

PI−PMMA copolymer	chromophore[a]	M_n[b] (PI/PMMA)	M_w^{uni}/M_n^{uni} [c]
I_{phe}-21	Phe	10.2K/46.6K	1.11
I_{an}-22	An	10.3K/54.9K	1.09
I_0-24		8.4K/48.7K	1.17

[a] Phe = phenanthrene (100% label density), An = anthracene (98% label density). [b] M_n is the number-average molecular weight (10K = 10 000) of the two blocks obtained from gel permeation chromatography (GPC) of the PI blocks in combination with ^1H NMR analysis of the block copolymer. [c] M_w^{uni}/M_n^{uni} values were determined from GPC measurements on the block copolymer.

Experimental Section

Materials and Sample Preparation. Acetonitrile (CH_3CN) and dichloromethane (CH_2Cl_2) (Aldrich, spectroquality) were used as received. Diblock copolymers of polyisoprene and poly(methyl methacrylate) (PI−PMMA), labeled at the block junction with either a fluorescent donor or acceptor chromophore, were synthesized by a multistep living anionic polymerization as described elsewhere.[28] The donor chromophore is phenanthrene (Phe), while the acceptor chromophore is anthracene (An). The donor-labeled copolymer is named I_{phe}-21 (I_{149}-MMA_{466}), where the subscripts refer to the number-averaged degree of polymerization of the blocks, and the acceptor-labeled copolymer is referred to as I_{an}-22 (I_{152}-MMA_{548}). An unlabeled PI−PMMA copolymer (I_0-24, I_{124}-MMA_{486}) of similar molecular weight and composition was also synthesized. The characteristics of the three diblock copolymers are summarized in Table 1.

The block copolymer solutions were prepared using two somewhat different methods. In the direct-dissolution method, acetonitrile was added to directly dissolve a solid block copolymer sample. Micellar solutions of the individual polymers prepared in this way could later be mixed to assess the rate at which the donor (D)- and acceptor (A)-labeled micelles would exchange their components. In the pretreatment method, the polymer sample was first dissolved in dichloromethane, a good solvent for both blocks. This solution was placed in a flask and concentrated under a stream of nitrogen to leave a thin film of polymer on the wall of the flask. The film was then dried under vacuum at 50 °C for 8 h in order to ensure a complete evaporation of the solvent. Acetonitrile was added to the flask to dissolve the polymer film. The pretreatment method was also used to prepare mixed micelles containing a binary blend of block copolymers. A mixture of two block copolymers was dissolved in dichloromethane and evaporated to form a thin film containing the two polymers. When this material was subsequently dissolved in acetonitrile, micelles were obtained containing both block copolymers. In this way we prepared samples in which the ratio of A-labeled to D-labeled polymer in the micelles could be controlled.

Micelles prepared using these two preparation methods differ in size, but as long as the samples were prepared using the same protocol, the results are reproducible and consistent. Unless it is specifically noted, all micellar solutions (labeled, unlabeled, and mixed) were prepared using CH_2Cl_2 as an intermediate step. In this way seven acetonitrile stock solutions of I_{phe}-21 and I_{an}-22 with a constant total copolymer concentration ($c_{tot.} = c_D + c_A = 0.25$ wt %) but with varying I_{an}-22 content were prepared. The weight ratios (w_A/w_D) are 0.25, 0.65, 1.01, 1.06, 1.26, 2.41, and 3.54. The copolymer I_{an}-22 has a labeling efficiency of 98%. Correcting for this, the weight ratios correspond to acceptor-labeled copolymer mole fractions, f_A, of 0.18, 0.36, 0.46, 0.47,

0.51, 0.67, and 0.74. The total mole fraction of I_{an}-22 is denoted $f_A^{tot.} = f_A/0.98 = n_A/(n_A + n_A(\text{unlabeled}) + n_D)$, where n_A is the number of moles of acceptor-labeled copolymer, n_D is the number of moles of donor-labeled copolymers, and n_A(unlabeled) denotes the number of moles of I_{an}-22 which are unlabeled. Micellar solutions containing only I_{phe}-21, I_{an}-22, or I_0-24 were also prepared. Each of the three single-component solutions had a polymer concentration 0.25 wt %.

Prior to the fluorescence decay measurements, the micellar solutions were deaerated by bubbling argon gas through them for 15−20 min. The samples were weighed before and after degassing to monitor possible solvent evaporation. The polymer solutions used in dynamic and static light scattering measurements and in viscosity measurements were filtered through Millipore 0.2 μm filters.

Viscosity Measurements. Viscosity measurements were performed using a Ubbelohde capillary viscometer (model C214 with a calibration constant of 0.000 992 mm^2/s^2) in a temperature-controlled water bath of 25.0 °C (temperature stability, ±0.01 °C). We examined four concentrations of the unlabeled PI−PMMA (I_0-24) in acetonitrile, in the range (0.145−0.292 wt %; 1.14−2.29 mg/cm^3). For the labeled system, containing mixed micelles of I_{phe}-21 and I_{an}-22 in a fixed weight ratio, $w_A/w_D = 1.01$, viscosity measurements were performed on six concentrations in the range (0.120−0.292 wt %; 0.943−2.30 mg/cm^3). The outflow times were always greater than 200 s, making kinetic energy corrections negligible. Acetonitrile was used as a reference. The specific viscosities ($\eta_{sp} = \eta_{rel} - 1$, where η_{rel} is the ratio of the solution to solvent outflow times) were plotted vs polymer concentration according to the Huggins equation:

$$\eta_{sp}/c = [\eta] + k_H[\eta]^2 c + ... \quad (1)$$

to obtain the intrinsic viscosity [η], where c is the weight concentration of block copolymer and k_H is the Huggins coefficient.

For the unlabeled I_0-24 micelles, [η] = 10.82 ± 0.02 cm^3/g was obtained from a weighted linear fit of the data to eq 1. Similarly, the intrinsic viscosity of the mixed micelles of I_{phe}-21 and I_{an}-22 is 12.04 ± 0.01 cm^3/g. The corresponding Huggins coefficients are 4.80 ± 0.07 and 0.83 ± 0.06, respectively. The large value of k_H for the I_0-24 micelles is unusual and is being investigated further.

Refractive Index Increment. The refractive index increment (dn/dc) of the unlabeled (I_0-24) and labeled copolymers (I_{phe}-21 and I_{an}-22) in acetonitrile were measured using a temperature controlled differential refractometer (KMX-16 from Milton Roy) with an internal He−Ne laser (632.8 nm) as a light source. The instrument was previously calibrated with NaCl solutions, giving a calibration constant $k' = 1.3498 \times 10^{-7}$. The reference was acetonitrile. Five I_0-24 concentrations were used, ranging in concentration from 0.0484 to 0.242 wt % (from 0.380 to 1.90 mg/cm^3), yielding a value of dn/dc = 0.143 ± 0.002 cm^3/g at 23 °C and 632.8 nm. The labeled copolymers (mixed in a fixed weight ratio of I_{an}-22 to I_{phe}-21 (w_A/w_D) = 1.01; concentrations of 0.009 73−0.146 wt % (0.0765−1.14 mg/cm^3)) gave a value of 0.141 ± 0.006 cm^3/g.

Due to the chemical heterogeneity of block copolymers, the weight-average molecular weight determined in static light scattering measurements is an apparent molecular weight. The corresponding dn/dc value for homo-PMMA in acetonitrile is obtained from literature as 0.140 cm^3/g.[40] The dn/dc values presented are the same as this literature value, and hence the measured apparent molecular weight is close to the true molecular weight.

Dynamic Light Scattering Measurements. Dynamic light scattering (DLS) experiments were performed in the homodyne mode using an argon-ion laser from Lexel Laser Inc. (model Excel 3000) operating at wavelength $\lambda = 488$ nm with adjustable output power. The output power was set depending upon the scattered intensity level of the sample. The solutions of copolymer in acetonitrile were filtered into 12.35 mm diameter glass scattering cells (from Brookhaven, BI RC 12) and placed in a Brookhaven goniometer equipped with a thermostated bath of liquid (toluene) which matched the refractive index of the glass cells. The detection device was a photomultiplier, the output of which was connected to the signal analyzer, a Brookhaven digital correlator (model BI-2030AT) with 136 linearly spaced channels, which produces the intensity time-correlation function, $g^{(2)}(t)$. $g^{(2)}(t)$ was measured at different scattering angles (θ) in the range of 45°−135°. The difference between the calculated and the measured baseline was always less than 0.08%. The temperature was set to 21 °C for all DLS measurements except for the experiments of the temperature dependence on the size of the unlabeled PI−PMMA micelles. The temperature was controlled to within ±0.01 °C.

Static Light Scattering Measurements. Intensity light scattering (SLS) measurements were performed on the unlabeled PI−PMMA (I_0-24) micelles in acetonitrile, as well as on the A- and D-labeled mixed micelles (weight ratio, $w_A/w_D = 1.01$). The experimental setup was the same as that for the DLS measurements, but a He−Ne laser (Spectra Physics model 127 operated at 632.8 nm) was employed instead of the argon-ion laser together with another pinhole size. The incident beam was vertically polarized, and the scattered beam was unpolarized. The reduced scattered intensity, $Kc/\Delta R_\theta$, was derived from the intensity measurements using the Brookhaven SLS software, where c is the block copolymer concentration. K is an optical constant containing the corresponding dn/dc value of each copolymer system (dn/dc(I_0-24) = 0.143 cm^3/g and dn/dc(I_{an}-22/I_{phe}-21) = 0.141 cm^3/g): $K = 4\pi^2 n_0^2(dn/dc)^2/(\lambda^4 N_{AV})$, where n_0 is the refractive index of the solvent. ΔR_θ is the excess Rayleigh ratio of the solution intensity to that of the solvent (acetonitrile) obtained through calibration using toluene as a reference: $R_{tol} = 1.40 \times 10^{-6}$ cm^{-1} (at 23 °C and 632.8 nm). The Rayleigh ratio is the intensity scattered in a given direction by a unit volume of solution, divided by the intensity of the incident light. For toluene, the scattered intensity multiplied by sin θ vs the angle was constant over the angular range of the experiments: 30°−150°.

Ultraviolet−Visible Absorption Measurements. Ultraviolet absorption measurements were made with a Perkin-Elmer Lambda 2 UV−vis double-beam spectrophotometer. Absorption spectra of the phenanthrene (D)- and anthracene (A)-labeled polymers were measured in a 1 cm quartz cell from which the background was subtracted by using the pure solvent (acetonitrile). For a I_{phe}-21 copolymer concentration of 0.25 wt % in acetonitrile, the absorption at 300 nm was 0.65, calculated from the baseline determined at 590 nm.

Steady-State Fluorescence Spectroscopy. Steady-state fluorescence measurements were carried out with a SPEX Fluorolog 212 spectrometer equipped with double-grating monochromators. Spectra were measured in steps of 1 nm and with an integrating time of 1 s. The slit widths were 1 mm for both excitation and emission. Both the sample signal (S) and a reference signal (R) for the lamp were recorded simultaneously and then divided to obtain S/R. Two types of experiments were

performed, donor fluorescence intensity measurements as a function of time (time-scan experiments) and fluorescence spectrum measurements. The spectrometer was used in a right angle configuration, and the absorbance at the excitation wavelength (λ_{ex}) was always less than 1.0.

For the time-scan measurements, a known weight and concentration of the donor-labeled (I_{phe}-21) micellar solution, prepared by direct dissolution in acetonitrile, was introduced in the cuvette and the fluorescence intensity was measured. Then, at $t = 0$, a known small volume of a concentrated solution containing only acceptor-labeled (I_{an}-22) micelles was pipetted directly into the cuvette. The donor emission wavelength (λ_{em}) was monitored at 348 nm, which corresponds to the secondary maximum in the phenanthrene emission spectrum, for samples excited at $\lambda_{ex} = 300$ nm. At first, the intensity from the sample solution was recorded every 120 s during a period of 2 h and compared to the intensity of a reference solution, which was the same as the initial solution (I_{phe}-21 in acetonitrile). After each measurement, the shutters were closed until the next pair of measurements were executed at a later time. This procedure was repeated over about 10 h. Thereafter a set of measurements (sample and reference) were made every day for a week.

Time-Resolved Fluorescence Spectroscopy. Fluorescence decay measurements were performed by the time-correlated single-photon-counting technique. A coaxial pulsed flash lamp from Edinburgh Instruments Ltd. (model 199F), working at 0.5 atm of D_2(g), was used as excitation source. All experiments were conducted with the excitation wavelength set to 300 nm, which corresponds to a maximum in the absorption spectrum of phenanthrene (the donor chromophore). The fluorescence emission was detected at right angle at 348 nm. To decrease the additional signal originating from light scattering, a cutoff filter with zero transmittance at 300 nm was placed in front of the photomultiplier. Data were analyzed by the MIMIC technique using *p*-terphenyl, with a fluorescence lifetime of 0.96 ns, as a reference. All experiments were carried out on deaerated solutions at room temperature (22−23 °C) with 20 000 counts collected in the maximum channel.

Data Analysis

Dynamic Light Scattering. If the scattered light obeys Gaussian statistics, the normalized time-correlation function of the electric field ($g^{(1)}(t)$) and the normalized measured intensity autocorrelation function ($g^{(2)}(t)$) are related by the Siegert relation:[41,42]

$$g^{(2)}(t) - 1 = \beta|g^{(1)}(t)|^2 \tag{2}$$

where t is the delay time and β (≤ 1) is a coherence factor which accounts for deviation from ideal correlation and is normally determined in the fitting procedure.

For polydisperse particle sizes, the electric field correlation function may be described by[43]

$$g^{(1)}(t) = \int_0^\infty \tau A(\tau) \exp(-t/\tau)\, \mathrm{d} \ln \tau \tag{3}$$

where τ is the relaxation time and $A(\tau)$ is the relaxation time distribution.

The DLS data were analyzed by regularized inverse Laplace transformation (RILT), to obtain the relaxation time distribution and the diffusion coefficients of the copolymer micelles (D). The RILT analysis uses the calculation algorithm REPES,[44] which is incorporated in the analysis package GENDIST.[5] It directly minimizes the sum of the squared differences between the experimental and the calculated $g^{(2)}(t)$ functions. A *probability to reject* parameter of 0.5 was chosen in all analyses. This factor makes the RILT analysis more robust to artifacts created by noise than most other data analysis techniques.[45] In the present study, a relaxation time distribution is presented in the form of $\tau A(\tau)$ vs $\log(\tau/\mu s)$, with $\tau A(\tau)$ in arbitrary units, providing equal area representation.

In the analysis, the relaxation rate of the correlation function or characteristic line width (Γ) is obtained from the first moment of the distribution. Γ is related to the translational diffusion process by the expression

$$D = (\Gamma/q^2)_{q\to 0} \tag{4}$$

where D is the translational mutual diffusion coefficient at a finite concentration, q is the magnitude of the scattering vector [$q = (4\pi n/\lambda)\sin(\theta/2)$], and λ is the wavelength of light in a vacuum. Here n is the refractive index of the solution, which for dilute solutions is taken to be the refractive index of the solvent.) D is obtained as the slope in a plot of Γ vs q^2, where Γ has been measured at different scattering angles.

From the diffusion coefficient at infinite dilution D_0, the hydrodynamic radius (R_H) of the copolymer micelles is calculated from the Stokes−Einstein relationship for noninteracting spheres:

$$R_H = kT/6\pi\eta_0 D_0 \tag{5}$$

where k is the Boltzmann constant, T is the absolute temperature, and η_0 is the solvent viscosity.

The DLS data were also fitted with a cumulant expansion,[46] included in the Brookhaven correlator software, the results of which were comparable with the RILT analyses. Also given in the cumulant fits is the variance or the width of the line width distribution function, μ_2/Γ^2, where Γ is the first cumulant and μ_2 is the second cummulant. μ_2/Γ^2 is a measure of the polydispersity in the size of the micelles.

Static Light Scattering. In a static light scattering experiment, one determines the reduced scattered intensity, $Kc/\Delta R_\theta$, where K is an optical constant defined above. ΔR_θ is the excess Rayleigh ratio of the solution. The reduced light intensity scattered from a dilute solution of large interacting macromolecules is expressed as

$$\frac{Kc}{\Delta R_\theta} = \frac{1}{P(\theta)}\left(\frac{1}{M_w} + 2A_2 c + ...\right) \tag{6}$$

where M_w is the apparent weight-average molecular weight and A_2 is the second virial coefficient. $P(\theta)$ is the form factor or particle scattering factor of the macromolecules, here the PI−PMMA micelles. The inverse of $P(\theta)$ is expressed as

$$P^{-1}(\theta) = \left(1 + \frac{16\pi^2 n_0^2 R_g^{\,2}}{3\lambda^2}\sin^2(\theta/2) + ...\right) \tag{7}$$

where R_g is the radius of gyration of the micelles. By extrapolation to zero angle, M_w and A_2 may be obtained from the concentration dependence of $Kc/\Delta R_\theta$. For each polymer concentration, an apparent R_g is obtained from the slope of the plot of $Kc/\Delta R_\theta$ versus $\sin^2(\theta/2)$.

Fluorescence Decay Profiles. Since the pioneering work of Förster,[47] many studies, both theoretical and experimental, have established that if certain experimental conditions are met, an electronically excited fluorescent molecule (donor D^*) may transfer its energy to another, nearby ground-state molecule

(acceptor A), forming D and A^* as byproducts. The rate of energy transfer $w(r)$ depends on the D−A separation distance r and is given by the expression

$$w(r) = \frac{(3/2)\kappa^2}{\tau_D^0}\left(\frac{R_0}{r}\right)^6 \quad (8)$$

where τ_D^0 is the lifetime of D^* in the absence of A. The constant R_0 depends on the spectroscopic characteristics of the pair; for most systems of interest it ranges from 2 to 6 nm.[48] When DET experiments are used to measure distances or distributions of distances, R_0 sets the distance scale of the measurements. The factor $3\kappa^2/2$ is related to the orientation of the transition moments of D^* and A. For the case of rapidly reorienting dipoles, the orientationally averaged value of this factor is exactly equal to unity. For most other situations lacking strong orientational correlations, this term falls within 10% of unity.[49] In this work we will assume that D and A chromophores at the solvent−core interface of a block copolymer micelle are sufficiently mobile that $3\kappa^2/2 = 1$.

In the Klafter−Blumen (KB) formulation,[50] all donors occupy equivalent positions, and the donor fluorescence decay curve, $I_D(t)$, can be expressed by a time-dependent function ($g(t)$) related to the energy-transfer process:

$$I_D(t) = I_D(0)\exp[-(t/\tau_D^0)]\exp[-g(t)] \quad (9)$$

The first exponential term on the right-hand side of eq 9 is the natural decay rate of D^* when no acceptors are present. The second term, $\exp[-g(t)]$, is the DET-related survival probability, i.e., the probability that an excited donor D^* will survive during a time interval of t without transferring energy to any neighboring acceptor molecule. The DET process leads to a nonexponential decay profile of $I_D(t)$ for which $g(t)$ may be written as

$$g(t) = p\int_V \rho(r)(1-\exp[-w(r)t])\,dV \quad (10)$$

where p, the probability that an acceptor molecule occupies a site where energy transfer may occur, is proportional to the acceptor concentration in the system. $\rho(r)$ is the site density distribution function, which depends on the geometry of the system, and V is the total volume in which DET can occur.

The KB methodology is based on the assumption of equivalent donor environments. When the donor and acceptor molecules are distributed in a Euclidean space of dimensionality Δ ($\Delta = 3, 2, 1$), the exponent function may be described by

$$g(t) = P(t/\tau_D^0)^\beta, \quad \beta = \Delta/6 \quad (11)$$

where P is a function of the acceptor concentration. Klafter and Blumen also showed that for donors and acceptors distributed on a fractal lattice, Δ is equal to the fractal (Hausdorff) dimension of the lattice. Equations 9−11 have also been applied to systems of restricted geometry, where fractional values of Δ are obtained, even though the system lacks the self-similar symmetry of a true fractal. Under these circumstances, β is sensitive to edge effects of the confining space, but Δ loses its meaning as a dimensionality of space.

In the present micellar system, the donor and acceptor chromophores are confined to the interface between the core and the corona of the micelle. If the micelle has a dense core comprising only the insoluble block and the interface is sharp, then DET will occur on the surface of a sphere of radius R_{core}; then $\beta = {}^1/_3$ ($\Delta = 2$), and eq 11 may be simplified to

$$g(t) = P\left(\frac{t}{\tau_D^0}\right)^{1/3} = f_A N_n^{agg}\frac{\Gamma(2/3)}{4}\left(\frac{R_0}{R_{core}}\right)^2\left(\frac{t}{\tau_D^0}\right)^{1/3} \quad (12)$$

where $\Gamma(2/3)/4 = 0.339$, f_A is the mole fraction of polymers with an acceptor at the junction (i.e. corrected with the acceptor label density), and N_n^{agg}, the aggregation number, is the mean number of block copolymer molecules in a micelle. It should be stressed that this equation is only valid when the micelle has a sharp interface, i.e., a strong segregation between the core block and the corona block, and is in a medium in which the solvent molecules have little solubility in the micelle core.

By fitting the experimental donor decay curves to eq 11, the micelle solutions containing different ratios of A- to D-labeled block copolymers, P and β values are obtained for each curve. Equation 11 predicts that β is independent of micelle composition and that P is proportional to f_A. Under these circumstances, a plot of P vs f_A should yield a straight line passing through the origin with the slope of $0.339N_n^{agg}(R_0/R_{core})^2$. Thus from the slope of this plot, the core radius of the micelles may be extracted.

Results

In acetonitrile, the PI−PMMA diblock copolymers form starlike micelles, with a PI core surrounded by a PMMA corona. When the micelles are prepared from block copolymers labeled with a fluorescent dye at the PI−PMMA junction, these dyes will be confined to the interface between the core and the corona of the micelles. For significant energy transfer to occur, both dyes must reside in the same micelle.

Steady-State Fluorescence Measurements. In Figure 1, fluorescence spectra are presented for two micelle samples in acetonitrile, prepared in different ways, containing the same weight ratio of I_{an}-22 and I_{phe}-21 ($w_A/w_D = 2.7$). Both samples were excited at $\lambda_{ex} = 300$ nm, a maximum of the Phe absorption. In these spectra, the Phe emission is detected from 345 to 360 nm, whereas the emission at $\lambda > 360$ nm is due to anthracene. The first sample was prepared by direct dissolution of each polymer separately in CH_3CN and then mixing of the solutions. One observes much less energy transfer (lower curve) than in the case of the second sample, where the polymers were first mixed in a common good solvent (dichloromethane), dried, and then dispersed in acetonitrile (upper curve) to yield mixed micelles. The first sample was monitored over time to see if an increase in the extent of energy transfer occurred. These measurements showed that no changes in the spectra occurred over a period of 1 week. We conclude that the exchange of block copolymer molecules between micelles is extremely slow.

Figure 2 displays the emission spectra of a series of molecularly mixed (I_{phe}-21 + I_{an}-22) micelles in acetonitrile. Also shown in the figure is the emission spectrum of the donor dye (phenanthrene) obtained from an acetonitrile solution containing only I_{phe}-21 micelles. The extent of DET increases strongly as the mole fraction of acceptor-labeled copolymer (f_A) in the mixed micelles increases from 0 to 0.740 (corrected values, $f_A = 0.98 \times f_A^{tot.}$).

Time-Resolved Fluorescence Measurements. Fluorescence decay profiles were measured for mixed micelles in acetonitrile ranging in composition from $w_A/w_D = 0.25$ to 3.54 ($f_A = 0-0.740$). Representative examples of these profiles were published in a previous communication.[28a] The analysis of these decay curves was carried out in two steps. First, the decay curves were fitted to eqs 9 and 11, with the donor lifetime fixed at the

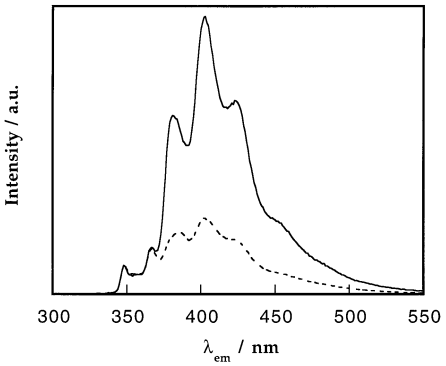

Figure 1. Fluorescence emission spectra for two PI−PMMA block copolymer micelle samples in acetonitrile, prepared in different ways, containing the same weight ratio ($w_A/w_D = 2.7$) of anthracene-labeled and phenanthrene-labeled PI−PMMA copolymers, I_{an}-22 and I_{phe}-21, respectively. The dashed line corresponds to the sample prepared by direct dissolution of each polymer separately in acetonitrile and then mixing the solutions. The solid line corresponds to the sample of mixed (I_{phe}-21 + I_{an}-22) micelles, i.e., I_{an}-22 and I_{phe}-21 randomly distributed in the same micelle. The excitation wavelength of the donor (Phe) is 300 nm. The spectra have been normalized at 348 nm, the emission wavelength of Phe.

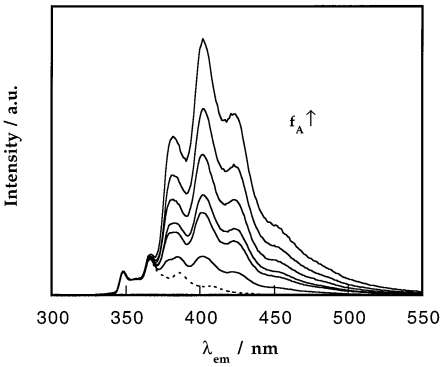

Figure 2. Fluorescence emission spectra of a series of mixed (I_{phe}-21 + I_{an}-22) micelles in acetonitrile with increasing increasing mole fraction of the acceptor-labeled copolymer, f_A. The dashed line corresponds to a sample of pure I_{phe}-21 micelles in acetonitrile. The total copolymer concentration is constant, $c_{tot.} = 0.25$ wt %. The excitation wavelength of the donor (Phe) is 300 nm. The spectra have been normalized at 348 nm, the emission wavelength of Phe.

unquenched value, $\tau_D^0 = 45.5$ ns. The three fitting parameters were the amplitude, $I_D(0)$, the P factor, and the exponent β. The goodness of the fit was examined through the random distribution of weighted residuals, the reduced χ^2, and the autocorrelation of the weighted residuals. The results of these fits are collected in Table 2. As may be noted, the fits are good, with $\beta = 0.345 \pm 0.034$, which corresponds to a dimensionality $\Delta = 2.07 \pm 0.20$ (eq 11).

These data were then reanalyzed by fixing the value of β to $^1/_3$, which corresponds to the assumption that DET takes place in two dimensions. With a reduced number of fitting parameters, one obtains better precision in the parameters fitted. These results are also presented in Table 2. The values of P, from which we derive information about the micelle core, are predicted in eq 12 to be proportional to the mole fraction of acceptors in the mixed micelles. In Figure 3, these P values are plotted as a function of the mole fraction of acceptor-labeled copolymers, f_A. We obtain a straight line which passes through the origin. The interpretation of these P values is deferred to the Discussion section of this paper.

Dynamic Light Scattering Measurements. Dynamic light scattering (DLS) measurements were performed on dilute acetonitrile solutions of I_0-24, I_{phe}-21, and I_{an}-22 and on the mixed micelles comprised of I_{an}-22 and I_{phe}-21 (with w_A/w_D ranging from 0.25 to 3.54). The intensity correlation functions obtained were single exponential in all cases. The data were analyzed using a regularized inverse Laplace transformation (RILT) which indicated monomodal relaxation time distributions. In Figure 4, an intensity correlation function (top) and its corresponding relaxation time distribution (bottom) from a typical DLS measurement are given. This result indicates that the PI−PMMA copolymers form solutions of well-defined micelles, in which the micelles are the single scattering entities and that no undefined aggregation occurs. Even at the lowest concentrations examined by DLS (see Figure 5) the critical micelle concentration (cme) of PI−PMMA copolymers in acetonitrile was not detected. We imagine that the cmc is extremely low due to the insolubility of the PI block in acetonitrile.

From the RILT analysis, we also obtain the relaxation rate (Γ) of the intensity correlation function. Γ was determined at different angles, for all concentrations ($c \leq 0.25$ wt %) of the different copolymers and copolymer mixtures investigated. In each instance, we obtained a linear plot, passing through the origin, of Γ vs the square of the scattering vector, q^2. This result indicates a diffusive process, and the translational diffusion coefficients (D) were calculated (eq 4) from the slopes of these plots. The diffusion coefficients exhibited no concentration dependence, as shown in Figure 5, where D as a function of

TABLE 2: Analysis of the Fluorescence Decay Profiles

weight ratio[a]	mole fraction[b]	P^c	β^c	$\chi^{2\,c}$	P^d	$\chi^{2\,d}$	R_{core} (nm)
0.25	0.175	0.509	0.434	1.02	0.653	1.20	(9.2 ± 0.9)
0.65	0.355	1.10	0.319	1.00	1.05	1.00	7.3 ± 0.7
1.06	0.470	1.38	0.357	1.11	1.46	1.14	7.7 ± 0.8
1.26	0.513	1.40	0.394	1.27	1.62	1.53	7.9 ± 0.8
2.41	0.666	2.15	0.307	1.29	1.99	1.33	7.5 ± 0.7
3.54	0.740	2.13	0.350	1.08	2.23	1.10	7.5 ± 0.8

[a] Weight ratio w_A/w_D of I_{an}-22 to I_{phe}-21 copolymers. [b] Mole fraction, corrected for 98% labeling of I_{an}-22, $f_A = 0.98 \times f_A^{tot.}$; $f_A^{tot.} = n_A/n_{tot.}$, where n_A and $n_{tot.}$ are the number of moles of the acceptor-labeled copolymer and the total number of moles of block copolymer, respectively. [c] P, β, and χ^2 were determined as fitting parameters (eqs 9−11) to the fluorescence decay profile. [d] P and χ^2 were determined by fitting the decay profiles with a fixed value of $\beta = {}^1/_3$.

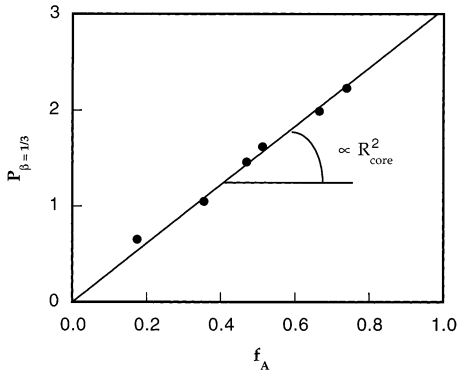

Figure 3. P factor as obtained from the fit of the fluorescence decay curves of the donor (Phe) emission to eq 12, as a function of the mole fraction of the acceptor-labeled copolymer (f_A) in the mixed (I_{phe}-21 + I_{an}-22) micelles in acetonitrile. The total copolymer concentration is constant, $c_{tot} = 0.25$ wt %. The excitation wavelength is 300 nm. In the analysis, the lifetime of Phe is fixed at 45.5 ns and β is fixed to $^1/_3$. The line is a weighted linear least-squares fit of P vs f_A. From the slope the core radius (R_{core}) is obtained; the slope $= 0.339 N_n^{agg}(R_0/R_{core})^2 = 3.05 \pm 0.05$.

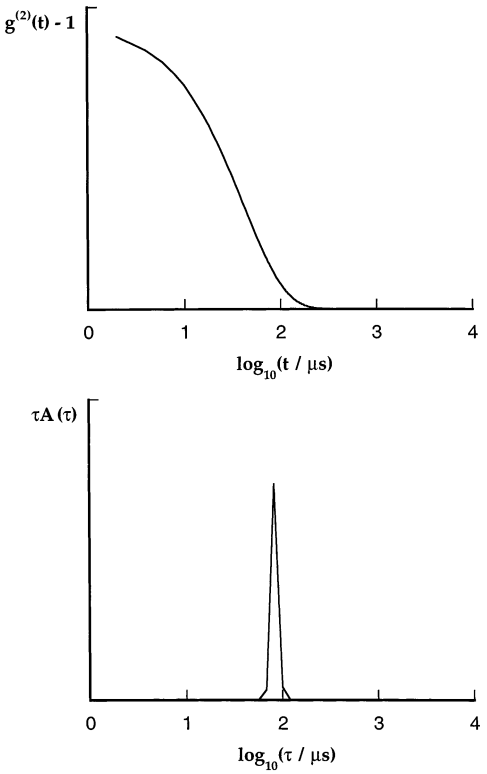

Figure 4. (Top) Intensity correlation function from a DLS measurement of PI−PMMA block copolymer micelles of I_{phe}-21 and I_{an}-22, molecularly mixed in a weight ratio $w_A/w_D = 3.54$. (Bottom) Corresponding relaxation time distribution obtained from inverse Laplace transformation of the DLS data. The total copolymer concentration in acetonitrile is $c_{tot.} = 0.10$ wt %.

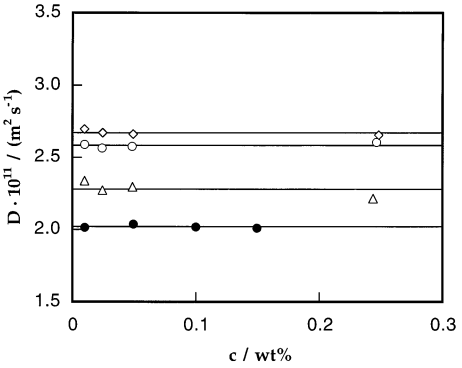

Figure 5. Apparent translational diffusion coefficients (D), from DLS measurements, of three different PI−PMMA block copolymer micelles in acetonitrile (donor-labeled, acceptor-labeled and unlabeled, I_{phe}-21, I_{an}-22, and I_0-24, respectively) as a function of copolymer concentration (c) at 21 °C. These micelles were prepared with the pretreatment method using dichloromethane as an intermediate step. The solid lines correspond to the average D values. From these, the hydrodynamic radii of the micelles are obtained as 21.6, 25.3, and 22.3 nm, for the I_{phe}-21 micelles (◇), I_{an}-22 micelles (Δ), and the I_0-24 micelles (○), respectively. For comparison, the D values of the I_0-24 micelles (●) prepared by direct dissolution in acetonitrile are also included.

total copolymer concentration is displayed for four PI−PMMA samples in acetonitrile. Thus, for all samples, D_0 is taken as the average value measured at several concentrations.

In Figure 5, the data for the I_0-24 micelles prepared by direct dissolution in CH_3CN are also presented. As may be noted, the diffusion coefficients are slower for this sample than those of the I_0-24 samples prepared from thin films cast from dichloromethane. A slower D corresponds to a larger hydrodynamic radius (R_H) (eq 5). This result provides evidence that the micelle size (and molecular weight) depend on the history of the sample preparation. Therefore, all the experimental results presented here, with the exception of those that examine the temperature dependence of R_H described below, are obtained for micelle solutions prepared via a common protocol, using dissolution in CH_2Cl_2 as an intermediate step.

TABLE 3: Hydrodynamic Radii from DLS Measurements [a]

f_A^{tot} [b]	R_H	f_A^{tot}	R_H
0[c]	21.6 ± 0.1	0.523[d]	24.73 ± 0.07
0.179	23.43 ± 0.04	0.755	25.26 ± 0.08
0.363	24.31 ± 0.09	1.0[e]	25.3 ± 0.6
0.467	25.2 ± 0.1	I_0−24	22.3 ± 0.1

[a] R_H in nanometers. [b] Mole fraction of I_{an}-22. [c] I_{phe}-21. [d] Corresponds to $w_A/w_D = 1.01$. [e] I_{an}-22.

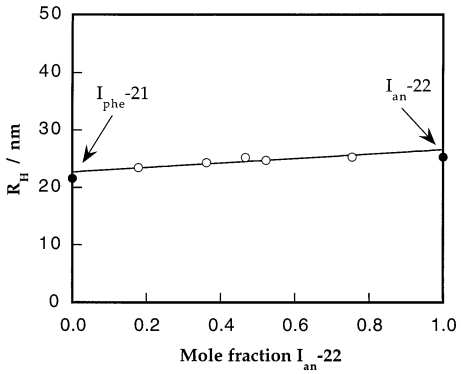

Figure 6. Hydrodynamic radius (R_H), from DLS measurements at 21 °C, of mixed (I_{phe}-21 + I_{an}-22) micelles in acetonitrile as a function of total mole fraction of I_{an}-22 ($f_A^{tot.}$) in the micelles. The solid line is a weighted linear least-squares fit.

Hydrodynamic radii of the micelles (at 21 °C) were calculated from the diffusion coefficients using the Stokes−Einstein equation (eq 5). These values are collected in Table 3 for the different types of PI−PMMA micelles. The R_H of the I_0-24, I_{phe}-21, and I_{an}-22 "pure" micelles are 22.3 ± 0.1, 21.6 ± 0.1, and 25.3 ± 0.6 nm, respectively. The hydrodynamic radii of the chromophore labeled micelles are plotted in Figure 6 as a function of the mole fraction of the I_{an}-22 copolymer ($f_A^{tot.}$). There is a small increase in R_H with an increasing amount of I_{an}-22 in the mixed micelles, consistent with the fact that I_{an}-22 has a longer PMMA block than I_{phe}-21, leading to a larger corona as the I_{an}-22 content increases.

Figure 7 displays the apparent hydrodynamic radius, $R_{H,app}$, of the I_0-24 micelles (prepared by direct dissolution in CH_3CN) at different temperatures ranging from 13.9 to 56.0 °C, which is below the boiling point of acetonitrile (81.6 °C). We conclude that there is an insignificant temperature dependence of the micellar radius. It is also likely, but not established, that exchange of copolymer molecules among micelles remains slow at 56 °C.

The size of the unimers (the individual copolymers) was also measured by DLS in good solvents, where no micelles are formed. The $R_{H,app}$ of the unlabeled copolymer I_0-24 in methyl acetate is 4.2 nm (at 25 °C, $c = 0.086$ wt %). A mixture of the labeled copolymers, I_{phe}-21 and I_{an}-22, in dichloromethane, gave an average $R_{H,app}$ value of 4.0 nm at 21 °C and at $c_{tot.} = 0.11$ wt %. The radii of the two individual labeled polymers were too close to be distinguished in these measurements.

Static Light Scattering Measurements. The apparent molecular weight (M_w), the second virial coefficient (A_2), and the radius of gyration (R_g) were determined by SLS at 21 °C for the unlabeled (I_0-24) micelles and for the molecularly mixed

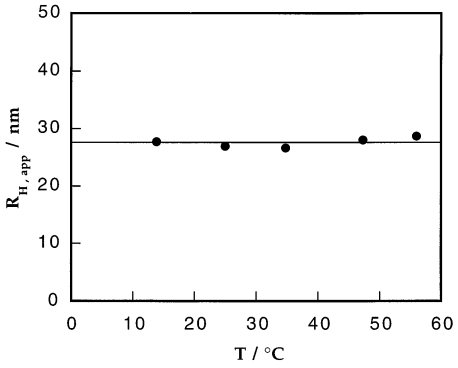

Figure 7. Apparent hydrodynamic radius ($R_{H,app}$) of unlabeled PI−PMMA (I_0-24) block copolymer micelles prepared by direct dissolution in acetonitrile at a concentration of 0.10 wt % as a function of temperature (T). The solid line corresponds to the average size.

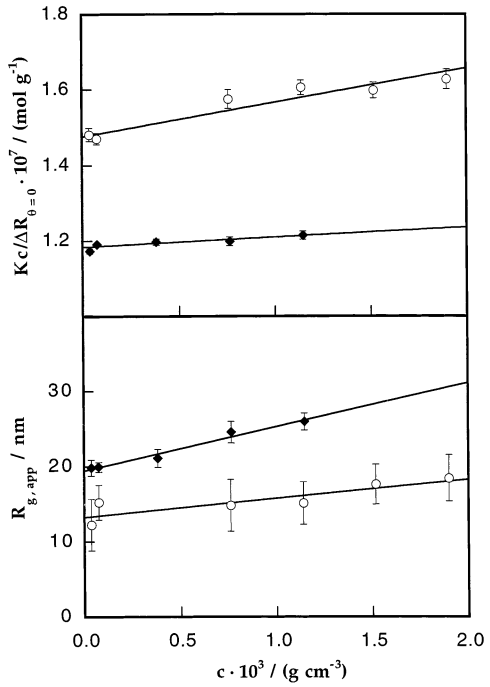

Figure 8. (Top) Reduced scattered intensity at zero scattering angle, $Kc/R_{\theta=0}$, obtained from SLS measurements at 21 °C, as a function of copolymer concentration (c) for unlabeled I_0-24 micelles (○) and mixed (I_{phe}-21 + I_{an}-22) micelles ($w_A/w_D = 1.01$) (♦) in acetonitrile. (Bottom) Apparent radius of gyration ($R_{g,app}$) for the same micelles, as a function of copolymer concentration (same symbols as top). The solid lines (top, bottom) are weighted linear least-squares fits to the SLS data.

(I_{phe}-21 + I_{an}-22) micelles ($w_A/w_D = 1.01$) in dilute acetonitrile solutions. For all I_0-24 solutions, a very weak angular dependence (at the limit of detection) of the reduced scattered intensity was observed over the whole experimental angular range. The $Kc/\Delta R_\theta$ values, extrapolated to zero angle ($\theta = 0$), as a function of I_0-24 concentration are shown in the top of Figure 8. Also displayed in the figure are the values for the mixed micellar system. From the intercepts ($Kc/\Delta\ R_{\theta=0,c=0}$), we calculate molecular weights of $(6.78 \pm 0.05) \times 10^6$ g/mol for the I_0-24 micelles and $(8.45 \pm 0.03) \times 10^6$ g/mol for the mixed micelles. The unimer molecular weight (M_w^{uni}) of the I_0-24 block copolymers is $(67 \pm 3) \times 10^3$ g/mol (Table 1). This is also the calculated average value of M_w^{uni} for this specific I_{an}-22/I_{phe}-21 mixture. Using these values, the weight-average aggregation numbers of the micelles are calculated. N_w^{agg} is equal to 101 ± 5 for the I_0-24 block copolymer micelles and 127 ± 6 for the I_{an}-22/I_{phe}-21 mixed micelles.

The second virial coefficients (eq 6) for the two systems were obtained from the slopes in Figure 8 (top): $A_2 = (4.5 \pm 0.6) \times 10^{-6}$ cm^3 mol^2/g for I_0-24 and $(1.3 \pm 0.5) \times 10^{-6}$ cm^3 mol^2/g for the mixed system. The virial coefficients obtained are small but positive and indicate that a small repulsive interaction exists between the micelles. As mentioned above, the cmc for these polymers is very low, and therefore the concentrations used in calculating micelle molecular weights from the SLS data have not been corrected for the cmc.

Although the angular dependence of the scattered light is rather weak, it was possible to estimate an apparent radius of gyration ($R_{g,app}$) of the two types of micelles. The $R_{g,app}$ values were calculated from the slopes of each corresponding concentration in the top of Figure 8 (see eq 6). The bottom of Figure 8 displays plots $R_{g,app}$ of the I_0-24 and the mixed micelles as a function of copolymer concentration. The radius of gyration at infinite dilution (R_g) is equal to 14 ± 2 nm for the I_0-24 micelles and 19.5 ± 0.6 nm for the mixed micelles. The larger error found for R_g of the I_0-24 micelles is due to a weaker angular dependence of the scattering intensity, and therefore a higher uncertainty in the determination of the slopes, compared to the I_{an}-22/I_{phe}-21 mixed micelles.

Viscosity Measurements. While R_H values were determined for all samples, viscosity measurements were carried out only on the micelle samples (I_0-24, and the ($w_A/w_D = 1.01$) mixed micelles of (I_{phe}-21 + I_{an}-22)) which were also examined by static light scattering. Intrinsic viscosity ([η]) values were calculated (eq 1) from the dependence of the reduced specific viscosity (η_{sp}/c) on total polymer concentration in CH_3CN. We obtained values of $[\eta] = 10.82 \pm 0.02$ cm^3/g for the unlabeled I_0-24 micelles, and 12.04 ± 0.01 cm^3/g for the mixed micelles. These small values indicate that the micelles are rather compact.

In the hard-sphere model, a viscometric radius (R_v) of the micelles may be estimated by combining the results from viscosity and SLS measurements.[51] R_v is then the radius of a hard sphere which exhibits the same intrinsic viscosity as that of the block copolymer micelle:

$$[\eta] = \frac{10\pi N_{AV} R_v^{\ 3}}{3M_v} \tag{13}$$

where M_v is the viscosity-average molecular weight, which for narrow mass distributions is essentially equal to M_w. N_{AV} is the Avogadro constant. Using the measured [η] and M_w values, R_v of the I_0-24 micelles and of the mixed micelles (w_A/w_D = 1.01) are found to be 22.65 ± 0.06 nm and 25.27 ± 0.03 nm, respectively.

Alternatively, from the relationship $[\eta] = 2.5/\rho_v$, where ρ_v is the density of the sphere in solution, the density of the micelles may be calculated.[52] We find for I_0-24 a density of 0.2311 ± 0.0003 g/cm^3. The corresponding value for the mixed micelles is 0.2077 ± 0.0002 g/cm^3.

More General DET Analysis. To evaluate the assumption of a flat interface between the micelle core and corona, we simulated a system in which the interface thickness could be varied. Since there is experimental evidence that the cores of PI−PMMA micelles are not swollen in acetonitrile,[28a] we assumed a distribution of junction points derived from the model of Helfand and Tagami for block copolymers in lamella domains,[53] modified to account for the spherical symmetry of the system:

$$P_J(r) = \frac{1}{n_J \cosh[2(r - R_{core})/\delta]} \tag{14}$$

where δ is the interface width, R_{core} is the radius of the micelle core, and n_J is a normalization constant. In the present case, this distribution has to be normalized over the micelle volume to account for the curvature of the core−shell interface, so that

$$n_J = 4\pi\int_0^\infty \frac{r^2}{\cosh[2(r - R_{core})/\delta]}dr \qquad (15)$$

Although the distribution function is assumed to have the same functional form as for a lamella structure, because we normalize the expression over $4\pi r^2$, it remains a good approximation even at high curvature radius ($R_{core} \approx \delta$).[29]

In a micelle solution of PI−PMMA diblock copolymers labeled at the junction of the two blocks with donors and acceptors, the fluorescence decay depends on the chromophore distribution in eq 14. The donor decay for Δ-pulse excitation will then be given by:[24−26]

$$I_D(t) = \exp[-(t/\tau_D^0)]\int C_D(r_D)\,\varphi(t,r_D) r_D^2\, dr_D \qquad (16a)$$

$$\varphi(t,r_D) = \exp\left[-\frac{2\pi}{r_D}\int_\infty^{R_e}(1 - \exp[-w(r)t])\left(\int_{|r_D-r|}^{r_D+r} C_A(r_A)\, r_A\, dr\right)r\, dr\right] \qquad (16b)$$

where τ_D^0 is the intrinsic fluorescence lifetime of the excited donor, $C_D(r)$ and $C_A(r)$ are the concentration profiles of donor and acceptor, and R_e is the cutoff radius. The donor concentration profile $C_D(r)$ can have any convenient concentration units, so we can use $C_D(r) = P_J(r)$. The acceptor concentration profile $C_A(r)$ must be a number density and therefore is given by $C_A(r) = n_A P_J(r)$, where n_A is the number of acceptor molecules in the micelle. For a dipole−dipole coupling mechanism the rate of energy transfer $w(r)$ between a donor and an acceptor separated by a distance r is given by eq 8.

Using a core radius of 7.6 nm, 73 acceptor molecules per micelle, $R_0 = 2.3$ nm, $\tau_D^0 = 45.5$ ns, and a time-scale of 1.04 ns/channel, we simulated decay functions for interface widths from 0 to 2.5 nm. The experimental fluorescence decay curve of mixed (I_{phe}-21 + I_{an}-22) block copolymer micelles (weight ratio, $w_A/w_D = 3.54$) in acetonitrile was fitted to each of the simulated decay curves, using a linear reconvolution algorithm. The fitting parameters are the decay normalization and the light scattering correction. To evaluate the quality of the fitting results, we calculated the reduced χ^2, the weighted residuals, and the autocorrelation of residuals.

The fitted decay curves for interface thicknesses of 0, 0.6, 0.9, and 1.1 nm are shown in Figure 9. From examination of the autocorrelation of residuals we can conclude from these decay curves that only the one that corresponds to a 0.9 nm interface yields a good fit. A plot of the reduced χ^2 vs interface thickness δ (Figure 10) shows that only for interface thickness values of 0.8−1.0 nm is it possible to obtain $\chi^2 < 1.5$ and evenly distributed autocorrelation of the residuals. For thicknesses smaller than 0.8 nm the reduced χ^2 is not very high ($\chi^2 \approx 2$), but the autocorrelation function shows a bias that indicates the inadequacy of the distribution. On the other hand, for thickness values greater than 1.0 nm there is no possible fit.

When the fluorescence decay profiles are fitted to eqs 9 and 12, which presume a sharp interface, good fits are obtained. From the fitting parameters, in conjunction with the assumption of a dense PI core, we calculate the aggregation number of the micelle and the core radius. However, when these same data are compared to simulated fluorescence decay profiles, which assume a Helfand-Tagami distribution of the junctions across the interface as well as an aggregation number for the micelles, we find that the interface is narrow but with a characteristic thickness of $\delta = 0.9$ nm.

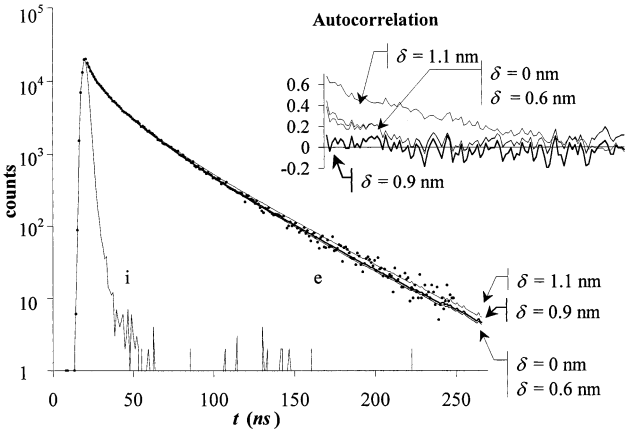

Figure 9. Experimental instrument response function (flash lamp), an experimental fluorescence decay curve of mixed (I_{phe}-21 + I_{an}-22) block copolymer micelles ($w_A/w_D = 3.54$) in acetonitrile, and fluorescence decay curves simulated using eqs 14−16 (for interface thicknesses of 0, 0.6, 0.9, and 1.1 nm) convoluted with the same instrument response function and fitted to the experimental decay curve. The autocorrelations of the corresponding residuals are also given.

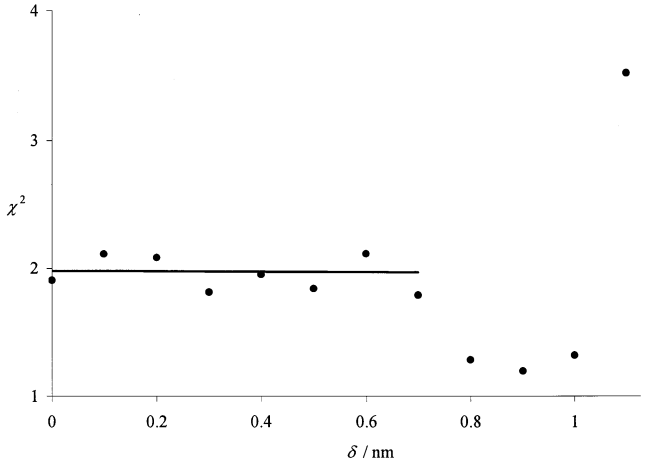

Figure 10. Plot of the reduced χ^2 parameter obtained for the fitting of the experimental fluorescence decay curve (same as in Figure 9) with increasing simulated interface thickness δ.

Discussion

Slow Exchange. In acetonitrile solution at room temperature, PI−PMMA micelles can be considered to be "frozen", although the PI micelle core is at a temperature well above the normal glass transition temperature of PI itself (−11 °C). Both DLS experiments, which show that micelle size depends on sample preparation protocol, and energy-transfer measurements indicate that the exchange rate of block copolymers among micelles is very slow. If the exchange occurs over a reasonable period of time, one can use DET measurements on mixtures of donor- and acceptor labeled micelles to follow the exchange process.[33,34] We were originally interested in carrying out such experiments, but the exchange rate for our micelles was too slow to be measured.

Frozen micelles are in fact rather common. The effect of preparation history on polystyrene-*b*-polybutadiene micelles in dimethylformamide (DMF) has been described by Riess and co-workers.[54] The authors found that the R_H of the micelles

prepared by direct dissolution of the polymer in DMF was larger than that prepared via dissolution first in a good solvent for both blocks, followed by dilution with DMF. Stejskal et al. also found size differences in their light scattering study of polystyrene-*b*-poly(ethylene-*co*-propylene) (PS−PEP) micelles in decane, which is a good solvent for PEP.[20] They suggested that when the block copolymers were dissolved from the solid, metastable micelles were formed with micellar cores preserved as formed from fracture of the morphology in the solid state. These nonequilibrium micelles had a larger R_H than those obtained after first heating the solution, followed by cooling. During this process, the micelles equilibrated with unimer at high temperature and then were trapped into a new frozen state when the solution was cooled to room temperature.

Polystyrene-*b*-poly(ethylene oxide) (PS−PEO) diblock copolymer micelles in water have been investigated using SAXS and DLS, where nonequilibrium or frozen micelles were found for the higher molecular weight block copolymers. Here the micelles were prepared via a dialysis technique, in which the micelles pass through an equilibrium with unimers at some composition of cosolvent and water.[21] Eisenberg et al. also reported nonequilibrium micelles of polystyrene-*b*-poly(acrylic acid) (PS−PAA) diblock copolymers in DMF that were dependent on the history of sample preparation.[1] Slow exchange has also been described in aqueous solution of poly(acrylic acid)-*b*-poly(methyl methacrylate) micelles, where energy-transfer experiments were used to distinguish between aggregated and molecularly dissolved states of the system.[55]

Micelle Size. Static light scattering experiments provide an aggregation number of 127 ± 6 for the mixed micelles of I_{an}-22 and I_{phe}-21 and 101 ± 5 for I_0-24. These are typical aggregation numbers for spherical starlike micelles formed by a block copolymer of this size and composition in a selective solvent. To obtain insights into the structure of the micelles, we compare their characteristic radii R_H, R_g, and R_v, obtained from DLS, SLS, and viscosity measurements, respectively. We first consider whether these micelles act as hard spheres. By definition, the model of impermeable rigid spheres presumes that $R_H = R_v$.[56] For both micellar systems, the hydrodynamic and viscometric radii are almost identical. The ratio R_v/R_H is 1.016 ± 0.007 for the I_0-24 micelles and 1.002 ± 0.005 for the I_{phe}-21/ I_{an}-22 ($w_A/w_D = 1.01$) mixed micelles. These micelles behave hydrodynamically like hard spheres.

A thermodynamic equivalent radius or hard-sphere virial radius (R_{A_2}) can be calculated from the second virial coefficient (A_2) and the apparent molecular weight (M_w) of the micelles.[57] R_{A_2} is a radius of a corresponding sphere where only the excluded volume effect has been taken into account:

$$R_{A_2} = \left(\frac{3M_w^2 A_2}{16\pi N_{AV}}\right)^{1/3} \qquad (17)$$

We calculate that R_{A_2} is 27 ± 1 nm for the I_0-24 micelles and 21 ± 2 nm for the mixed micelles. Noninteracting spherical particles should have a thermodynamic radius, R_{A_2}, equal to R_v (and to R_H). For both PI−PMMA micelles, the values of R_{A_2} obtained from the SLS measurements are fairly close to those of R_v and R_H, but not identical.

Another way of expressing the relationship between R_{A_2} and R_v for a hard sphere is that the ratio $A_2M_w/[\eta]$ should be equal to 1.6.[58] The experimental values found here are 2.8 ± 0.4 and 0.9 ± 0.3 for the unlabeled and labeled mixed PI−PMMA micelles, respectively. This comparison of results from SLS and viscosity measurements implies that the copolymer micelles may be considered hydrodynamically as compact spheres, although the interaction potential between the micelles is not purely repulsive, as one would expect for noninteracting hard spheres. This is the type of result one would expect for starlike block copolymer micelles, where the corona chains create a "soft" surface. Starlike micelles will have a softer repulsion than brushlike or crew-cut micelles.

The ratio of the radius of gyration to the hydrodynamic radius (R_g/R_H)[59] also provides information on the internal morphology of the PI−PMMA micelles. For a Gaussian linear chain, $R_g/R_H = 1.29$, whereas for a perfect homogeneous sphere, $R_g/R_H \leq 0.775$.[56] The I_0-24 micelles have a value of $R_g/R_H = 14/22.3 = 0.63 \pm 0.09$, and the mixed micelles of I_{phe}-21 and I_{an}-22 have $R_g/R_H = 19.5/25.2 = 0.77 \pm 0.02$. Both values are lower than the hard-sphere value. Antonietti has explained that R_g/R_H will be lower than 0.775 for a sphere with a soft corona surface.[3,60] Qin et al. also reported small values of this radius for PS−PMMA block copolymer micelles in a mixed solvent.[58] For these micelles, R_g/R_H varied from 0.39 to 0.59, and the authors interpreted their data in terms of a model of concentric spheres with either a "dry" or a swollen core.

Gast et al. reported a light scattering study of PS−PEO diblock copolymer micelles in water-saturated cyclopentane in which they found R_g/R_H ratios between 0.70 and 0.75.[16a] The results were interpreted in terms of a starlike micelle model (a density distribution model). The authors explained that for a core-free star molecule under Θ conditions, $R_g/R_H = 0.707$. When the aggregation number of the PS−PEO micelles increased to about 100, the R_g/R_H ratio reached a value of 0.77, which is between that of a solid sphere (0.775) and a star (0.707). The very low value ($R_g/R_H \approx 0.6$) we find for the I_0-24 micelles may be due in part to the large uncertainty of the radius of gyration for this sample. We note that even smaller values of R_g/R_H ratios, in the range 0.53−0.75, have been reported by Riess and co-workers, from a combination of small-angle X-ray scattering (SAXS) and DLS measurements on PS−PEO micelles in water.[21] The results presented here on the PI−PMMA/CH_3CN systems are thus reasonable when compared to other results reported in the literature on similar starlike block copolymer micellar systems.

Further information about the shape of the PI−PMMA micelles in acetonitrile may be obtained by evaluating the Mandelkern−Flory−Scheraga parameter, β_{MFS}. This parameter includes the ratio of the micellar radii obtained from viscosity measurements and DLS:[60]

$$\beta_{MFS} = \frac{(M_w[\eta])^{1/3}}{6\pi R_H} = \frac{R_v}{R_H}\frac{(10\pi N_{AV}/3)^{1/3}}{6\pi} \qquad (18)$$

$\beta_{MFS} = 9.80 \times 10^6$ mol$^{-1/3}$ for a hard impermeable sphere (since $R_v/R_H = 1$). For linear polymers, the theoretical β_{MFS} values are 10.49×10^6 mol$^{-1/3}$ for nondraining chains in good solvent ($R_v/R_H = 1.03$) and 10.10×10^6 mol$^{-1/3}$ for unperturbed chains (Θ condition) ($R_v/R_H = 1.07$).[56,61] The experimental β_{MFS} values obtained in this work are (9.96 ± 0.07) × 10^6 (I_0-24 micelles) and (9.82 ± 0.05) × 10^6 mol$^{-1/3}$ (mixed micelles). Both β_{MFS} values are closer to the value expected for hard spheres. In summary, our data on these PI−PMMA micelles in acetonitrile are consistent with starlike spherical micelles with a dense core and a soft solvent-swollen corona.

Micellar Aggregation Number. Micelle molecular weights and aggregation numbers can be determined directly from Zimm plots of the SLS data and from a comparison of the intrinsic viscosity and diffusion coefficient of the micelle with the help

of the hard-sphere model. Aggregation numbers are also available indirectly from DET measurements on the donor- and acceptor-labeled mixed micelles. When the data from these two sets of measurements are compared, information about the size and composition of the micelle core can be obtained. We begin with a discussion of the intrinsic viscosity and light scattering results.

From light scattering. Equation 13 can be used to calculate the molecular weights of the micelles from intrinsic viscosity and R_H values by setting $R_H = R_v$, i.e., by assuming that the micelles behave hydrodynamically like hard spheres. For I_0-24 micelles, we obtain $M_{cal} = (6.5 \pm 0.1) \times 10^6$ g/mol which is similar in value to $M_w = (6.78 \pm 0.05) \times 10^6$ g/mol determined by static light scattering. For the micelles comprised of (I_{phe}-21 + I_{an}-22) in a weight ratio of 1.01, we calculate $M_{cal} = (8.4 \pm 0.1) \times 10^6$ g/mol, similar to the SLS value $M_w = (8.45 \pm 0.03) \times 10^6$ g/mol. From the weight-averaged unimer molecular weight, M_w^{uni}, and M_w for the micelles, we calculate weight-averaged aggregation numbers of $N_w^{agg} = 101 \pm 5$ for I_0-24 micelles and $N_w^{agg} = 127 \pm 6$ for the 1:1 mixed micelles of (I_{phe}-21 + I_{an}-22).

From DET measurements. Energy-transfer rates for donors and acceptors distributed on the surface of a small sphere comparable in size to R_0 are sensitive to the radius of the sphere. If this sphere is the core of a block copolymer micelle, the P value (eq 12) obtained by fitting the donor decay profile is proportional to the number-average micelle aggregation number and the inverse square of the core radius [$P \sim f_A N_n^{agg}(R_0/R_{core})^2$]. The data in Figure 3 show that this prediction is satisfied over a wide range of f_A values. To separate these variables, one can either introduce independently determined values of the aggregation number or make an assumption about the composition of the micelle core.

The calculated slope of the line in Figure 3 is $0.339N_n^{agg} = 3.05 \pm 0.05$. Assuming a spherical core composed only of PI, the aggregation number may be expressed as

$$N_n^{agg} = \frac{4\pi R_{core}^{\ 3} \rho_{PI} N_{AV}}{3M_n^{PI}} \qquad (19)$$

where M_n^{PI} is the number-average molecular weight and ρ_{PI} is the density of the PI core. Combining these two expressions, and using the average of the PI blocks of the two labeled copolymers $M_n^{PI} = (10.3 \pm 0.6) \times 10^3$ g/mol, and the PI bulk density, $\rho_{PI} = 0.913$ g/cm^3, a core radius of $R_{core} = 7.6 \pm 0.8$ nm is calculated. The number of polymer molecules in a PI−PMMA micelle with a core radius of 7.6 nm is $N_n^{agg} = 98 \pm 22$. The large uncertainty in this value is due primarily to the uncertainty in the magnitude of R_0 (2.3 ± 0.1 nm). The value of N_n^{agg} is close to, but smaller than, the value $N_w^{agg} = 127 \pm 6$.

A core radius for each mixed micelle sample in the series can also be calculated from the individual fluorescence decay curves. With the assumption that the core has the same density as bulk PI, R_{core} is related to the fitting parameter P and the sample composition f_A by the expression

$$R_{core} = \frac{(P/f_A)\bar{M}_n^{PI}}{0.339(4\pi)\,\rho_{PI} R_0^{\ 2} N_{AV}} \qquad (20)$$

where $f_A > 0$ and $\bar{M}_n^{PI} = [f_A^{tot.} M_A^{PI} + (1 - f_A^{tot.}) M_D^{PI}]$ is the mean molecular weight of the PI blocks in each mixed micelle. $M^{PI}{}_A$ and $M^{PI}{}_D$ are the molecular weights of the PI block in I_{an}-22 and I_{phe}-21, respectively. R_{core} values calculated in this way are presented in Table 2. For the sample with $f_A = 0.175$, the extent of energy transfer is very small, and the decay profile deviates only slightly from an exponential form. As a consequence, there is little accuracy in the value of P determined for this sample. The other individual R_{core} values are scattered around the value obtained previously from the slope in Figure 3, which represents the average value of the core radius of these mixed micelles.

The labeled copolymers, I_{phe}-21 and I_{an}-22, have different PMMA block lengths. Because the values of R_{core} from the various mixtures of (I_{phe}-21 + I_{an}-22) are indistinguishable, we conclude that, within experimental error, the core radii and aggregation numbers of the micelles are independent of the composition of the mixture, and the difference in PMMA block lengths is not sufficient to cause a significant difference in micelle aggregation numbers. Two different averages of the aggregation numbers are determined by the different experimental methods: from DET we obtain N_n^{agg}, whereas SLS yields N_w^{agg}. Assuming that $N_n^{agg} = 98$ corresponds to the mixed micelle with $w_A/w_D = 1.01$, we calculate a ratio of $N_w^{agg}/N_n^{agg} = 1.3$.

We can also obtain a measure of micelle polydispersity from the DLS measurements. The second cumulant, μ_2, from the cumulant analysis of the correlation functions from dynamic light scattering measurements, is related to the polydispersity of the sample, μ_2/Γ^2.[62] We find that μ_2/Γ^2 varies between 0.014 and 0.059 for the micelle samples investigated. Assuming a log-normal molecular weight distribution, for which $M_z/M_w = M_w/M_n$, we calculate micelle polydispersities of $M_w/M_n = 1.1$ to 1.2.[3] Values of the same order of magnitude are obtained by using instead the approximation $\mu_2/\Gamma^2 \approx (M_w/M_n - 1)/4$ (Gaussian coils) or $\mu_2/\Gamma^2 \approx (M_w/M_n - 1)/9$ (hard spheres): $M_w/M_n = 1.1$ to 1.2 and $M_w/M_n = 1.1$ to 1.5, respectively.[43,44] Considering the error in N_n^{agg}, these micellar polydispersity indices are in reasonable agreement with each other.

In the RILT analysis of the dynamic light scattering data, narrow widths of the relaxation time distributions are obtained, corresponding to even lower values than those obtained from the cumulant analysis: 0.007−0.034. Fits of the Williams−Watts function to the various experimental correlation functions may also give a measure of the width of the relaxation time distributions, in the form of the β^{ww} factor ($0 < \beta^{ww} \leq 1$, where 1 corresponds to a perfect single-exponential curve).[63] Here we obtain narrow distributions with β^{ww} factors no lower than 0.95. These values together with those obtained from the RILT analysis provide indirect evidence that the size distribution of the PI−PMMA block copolymer micelles is narrow.

Micelle Corona. Acetonitrile is not a particularly good solvent for PMMA at room temperature. PMMA synthesized by anionic polymerization in tetrahydrofuran (THF) is predominately syndiotactic. Reports in the literature identify the Θ temperature for PMMA in CH_3CN at approximately 44 °C. For example, from SLS measurements, Yamakawa and co-workers found a Θ temperature for s-PMMA of 44 °C, which is identical to the Θ temperature for atactic PMMA (a-PMMA) in the same solvent.[64] Our experiments were carried out at 20 °C below this value. If the solvent medium for the PMMA corona chains is poorer than a Θ solvent, one would expect the corona thickness to be smaller than the unperturbed dimensions of the PMMA molecules and would expect a net attraction between micelle pairs. Nevertheless, stable micelles are formed, and a positive second virial coefficient is found in the static light scattering experiments. This behavior in contradiction to expectations makes it worthwhile to examine the properties of the micelle corona in more detail.

TABLE 4: PI−PMMA Micelles in Acetonitrile. Experimental and Theoretical Values of the Corona Length [a]

					L_c^{calc}		error (%)	
$f_A^{tot.}$	R_H	N_{MMA}[b]	N[c]	L_c[d]	DD[e]	DB[e]	DB	DB
0.179	23.4	481	137	15.8	16.6	16.2	5	2
0.363	24.3	496	142	16.7	17.0	16.5	2	1
0.467	25.2	504	144	17.6	17.1	16.7	3	5
0.523	24.7	509	145	17.1	17.2	16.8	1	2
0.755	25.3	528	151	17.7	17.7	17.1	0	3

[a] R_H and L_c in nanometers. [b] Average PMMA block length for the mixed micelles. $N_{MMA} = 548$ and 466 for I_{an}-22 and I_{phe}-21, respectively. [c] Obtained from $L_c = R_H - R_{core}$. The error in L_c is 0.8 nm. [d] Number of statistical segments in PMMA block: $N = N_{MMA}/3.5$. [e] DD = density distribution model (eq 21); DB = discrete blob model (eq 22). The following values are used in the calculations: $R_{core} = 7.6$ nm; $N_n^{agg} = 98$; $\nu = 0.5$; $a = 1.08$ nm.

We calculate values for the hydrodynamic corona thickness (L_c) from the expression $L_c = R_H - R_{core}$, using a common value of $R_{core} = 7.6$ nm for I_{phe}-21, I_{an}-22, and their mixtures. As seen in Figure 6, there is a small increase in L_c with increasing amounts of I_{an}-22, which parallels the increase in R_H, and follows from the fact that the I_{an}-22 copolymer has a longer PMMA block than I_{phe}-22. Values of L_c calculated in this way vary from 15.8 to 17.7 nm (Table 4).

Since acetonitrile is not a good solvent for PMMA, we compare the corona thickness with the unperturbed dimensions of PMMA. The root-mean-square end-to-end distance, $\langle r^2\rangle_0^{1/2}$, of a PMMA chain can be calculated from the characteristic ratio, $C_\infty = \langle r^2\rangle_0/nl^2$,[65] where n is the number of bonds in the chain and l is the bond length (l varies from 0.153 to 0.154 nm [65−67]). Values of $C_\infty = 7.3$ [68] and 7.5 [69] for s-PMMA are found in the literature. From these values, we calculate $\langle r^2\rangle_0^{1/2} \approx 13$ nm for the PMMA chain of I_{phe}-22, and 14 nm for that of I_{an}-22. Alternatively, we can use the empirical relation between R_g^w and M_w for s-PMMA ($R_g^w/M_w^{1/2}$)[70] to calculate R_g^w values of 5.5 and 5.9 nm, respectively, for the PMMA chains of the two polymers. After a small correction for sample polydispersity, we find $R_g^z = 5.7$ nm for I_{phe}-22 and 6.1 nm for I_{an}-22.[71] Since $\langle r^2\rangle_0 = 6(R_g^w)^2$, we calculate values of $\langle r^2\rangle_0^{1/2} \approx 13-14$ nm for these two polymers. From this exercise, we learn that the corona thickness is comparable or slightly larger than the root-mean-square end-to-end distance of PMMA of comparable length and significantly larger than the unperturbed radii of gyration of these chains.[72]

This type of behavior is more typical of starlike micelles in a good solvent for the corona chains. For example, Brown et al. found that the corona thickness was larger than the unperturbed dimensions of polystyrene-*b*-poly(dimethyl siloxane) (PS−PDMS) diblock copolymer micelles in *n*-dodecane, which is a relatively good solvent for PDMS.[73] A number of authors have discussed the effect of solvent quality on the corona thickness. The quality of the solvent will also influence the amount of stretching of the corona chains. This effect has been discussed for other micellar systems.[1,4b,36] Liu et al. have shown that as cyclohexane is added to a solution in tetrahydrofuran of starlike micelles with PS corona chains, the hydrodynamic radius of the micelle decreases. THF is a good solvent for PS at room temperature, whereas cyclohexane is a poor solvent (Θ temperature = 34.5 °C).[36]

Another parameter which will influence the degree of extension of the PMMA corona chains is the surface or interface area per corona chain, *s*; see for example ref 1 and references cited therein. The chains in the corona are in a semidilute condition, and a high surface density will promote stretching of the corona chains. This area can be calculated from the core radius and the aggregation number: $s = 4\pi R_{core}2/N_n^{agg}$, where we use $R_{core} = 7.6$ nm and $N_n^{agg} = 98$ as the number-averaged degree of aggregation. We find $s = 7.4$ nm^2, implying a separation between junctions of approximately 3.1 nm. An even smaller separation would be calculated if we used the $N_w^{agg} = 127$ determined from light scattering. Alternatively, the surface density of the corona chains σ ($\equiv 1/s$) could be used. The surface density above which the corona chains are overlapping is given by $\sigma_{ol} = 1/(\pi R_g^2)$, where R_g is the radius of gyration of the free corona homopolymer in solution.[74] In this case, using the radii obtained above, the ratio σ/σ_{ol} is $\gg 1$. This implies that the separation between junctions is less than the average distance extension of the PMMA homopolymer in solution and therefore the corona chains are stretched. Or, equivalently, since the PI−PMMA micelles we examine satisfy the condition $s^{1/2} < R_g$, coil overlap leads to stretching of the corona chains.

Expressions can be found in the literature for calculating the corona thickness of starlike micelles, using the corona chain length, expressed as the number of monomers per statistical segment (N), the statistical segment length (a), and the micelle aggregation number as input parameters. In the discrete blob (DB) model of d'Oliviera et al., the appropriate expressions are[19b]

$$L_c^{DB} = \left[Na^{1/\nu}\frac{(1+2\Xi)^{1/\nu}-1}{(2\Xi)^{1/\nu}} + R_{core}^{1/\nu}\right]^{\nu} - R_{core}$$

$$\Xi = \frac{2\sin(\gamma/2)}{1-\sin(\gamma/2)}$$

$$\cos\gamma = \left(\frac{\cos\alpha}{1-\cos\alpha}\right)$$

$$\alpha = \pi\frac{N_n^{agg}+2}{3N_n^{agg}} \qquad (21)$$

Here, Ξ is defined as the ratio between the diameter of the first polymer chain blob in the corona and the radius of the micelle core. N is the number of statistical segments in the PMMA chain. For PMMA, there are 3.5 monomers per segment, i.e., $N = N_{MMA}/3.5$ (N_{MMA} is the number of MMA units). The MMA monomer length is 2×0.154 nm $= 0.308$ nm, so the statistical segment length, a, is 3.5×0.308 nm $= 1.08$ nm.[66]

In the density distribution (DD) model of Vagberg and Gast, the corresponding expression is[16a]

$$L_c^{DD} = \left[Na^{1/\nu}\frac{8(N_n^{agg})^{(1-\nu)/2\nu}-1}{4^{1/\nu}(3\nu)} + R_{core}^{1/\nu}\right]^{\nu} - R_{core} \qquad (22)$$

Using $\nu = 0.5$, appropriate for a Θ solvent, and $a = 1.08$ nm for PMMA, we calculate theoretical corona thicknesses (L_c^{calc}) from eq 21 and eq 22 for the mixed micelles of (I_{phe}-21 + I_{an}-22). The values are presented in Table 4 in addition to the measured L_c values. The theoretical corona thicknesses, calculated using the DD model, are in good agreement with the experimental values. The calculated DB model values are somewhat larger than the measured values but still in a reasonable agreement.

Summary

PI−PMMA block copolymers with a long PMMA block form spherical starlike micelles in acetonitrile solution. Viscosity measurements in combination with static and dynamic light

scattering experiments establish the structure of the micelles as spheres with a dense core and a soft solvent-swollen corona that behave hydrodynamically as hard spheres. Energy-transfer experiments on micelles prepared from junction-labeled block copolymers (ca. I_{150}-MMA_{500}) provide the core radius (7.6 ± 0.8 nm) and the number-averaged aggregation number (N_n^{agg} = 98 ± 22), with the largest contributor to the uncertainty in this value being the small estimated uncertainty (± 0.1 nm) in the Förster radius R_0. A more sophisticated analysis of the energy-transfer data in terms of simulated fluorescence decay profiles suggest that the interface is narrow, but with a characteristic thickness of 0.9 nm. These simulations assume a Helfand−Tagami distribution of the block copolymer junctions across the interface. SLS experiments provide the weight-averaged aggregation number; here N_w^{agg} = 127 ± 6. It is interesting to note that the ratio of N_n^{agg}/N_w^{agg} = 1.3 is very close to the size polydispersity determined from a cumulant analysis of the DLS data for these micelles.

Acknowledgment. The authors thank NSERC Canada and the donors of the Petroleum Research Fund, administrated by the American Chemical Society, for their support of this work. K. S. would like to thank the Swedish Natural Science Research Council (NFR) for a fellowship supporting her stay in Toronto. J. P. S. F. Farinha acknowledges the support of FCT-PRAXIS XXI. We thank Dr. Robert M. Johnsen for providing the GENDIST program.

Appendix

The error analysis of the results were performed according to the following standard equations:

$$A = x \pm y \pm z$$

$$\Delta A = \pm[(\Delta x)^2 + (\Delta y)^2 + (\Delta z)^2]^{1/2} \quad \text{(A1)}$$

$$A = xy/z$$

$$\Delta A = \pm A[(\Delta x/x)^2 + (\Delta y/y)^2 + (\Delta z/z)^2]^{1/2} \quad \text{(A2)}$$

$$A = y^n$$

$$\Delta A = \pm A\frac{n\Delta y}{y} \quad \text{(A3)}$$

References and Notes

(1) Zhang, L.; Barlow, R. J.; Eisenberg, A. *Macromolecules* **1995**, *28*, 6055−6066.

(2) Moffitt, M.; Zhang, L.; Khougaz, K.; Eisenberg, A. In *Solvents and Self−Organization of Polymers*; NATO ASI Series, Vol. 327; Webber, S. E., Munk, P., Tuzar, Z., Eds.; Kluwer Academic Publishers: Dordrecht, The Netherlands, 1996; pp 53−72.

(3) Antonietti, M.; Heinz, S.; Schmidt, M.; Rosenauer, C. *Macromolecules* **1994**, *27*, 3276−3281.

(4) (a) Zhang, L.; Eisenberg, A. *Science* **1995**, *268*, 1728−1731. (b) Yu, Y.; Zhang, L.; Eisenberg, A. *Macromolecules* **1998**, *31*, 1144−1154.

(5) Schillén, K.; Brown, W.; Johnsen, R. M. *Macromolecules* **1994**, *27*, 4825−4832.

(6) Tao, J.; Stewart, S.; Liu, G.; Yang, M. *Macromolecules* **1997**, *30*, 2738−2745 and references cited therein.

(7) Price, C.; Chan, E. K. M.; Hudd, A. L.; Stubbersfield, R. B. *Polym. Commun.* **1986**, *27*, 196−198.

(8) Tuzar, Z.; Kratochvíl, P. In *Surface and Colloid Science*, Vol. 15; Matijevic, E., Ed.; Plenum Press: New York, 1993; pp 1−83.

(9) Gast, A. P. *Curr. Opin. Colloid Interface Sci.* **1997**, *2*, 258−263.

(10) *Solvents and Self-Organization of Polymers*; NATO ASI Series, Vol. 327, Webber, S. E., Munk, P., Tuzar, Z., Eds.; Kluwer Academic Publishers: Dordrecht, The Netherlands, 1996.

(11) For aqueous block copolymer systems, see for example: (a) Almgren, M.; Brown, W.; Hvidt, S. *Colloid Polym. Sci.* **1995**, *273*, 2−15. (b) Chu, B. *Langmuir* **1995**, *11*, 414−421. (c) Alexandridis, P. *Curr. Opin. Colloid Interface Sci.* **1996**, *1*, 490−501.

(12) (a) Nguyen, D.; Williams, C. E.; Eisenberg, A. *Macromolecules* **1994**, *27*, 5090−5093. (b) Moffitt, M.; Yu, Y.; Nguyen, D.; Graziano, V.; Schneider, D. K.; Eisenberg, A. *Macromolecules* **1998**, *31*, 2190−2197.

(13) Mortensen, K.; Brown, W.; Almdal, K.; Alami, E.; Jada, A. *Lanmuir* **1997**, *13*, 3635−3645.

(14) Hickl, P.; Ballauff, M.; Jada, A. *Macromolecules* **1996**, *29*, 4006−4014.

(15) (a) Xu, R.; Winnik, M. A.; Hallet, F. R.; Riess, G.; Croucher, M. D. *Macromolecules* **1991**, *24*, 87−93. (b) Xu, R.; Winnik, M. A.; Hallet, F. R.; Riess, G.; Chu, B.; Croucher, M. D. *Macromolecules* **1992**, *25*, 644−652.

(16) (a) Vagberg, L. J. M.; Cogan, K. A.; Gast, A. P. *Macromolecules* **1991**, *24*, 1670−1677. (b) Cogan, K. A.; Gast, A. P.; Capel, M. *Macromolecules* **1991**, *24*, 6512−6520.

(17) Daoud, M.; Cotton, J. P. J. Phys. **1982**, *43*, 531−538.

(18) Halperin, A. *Macromolecules* **1987**, *20*, 2943−2946.

(19) (a) d'Oliviera, J. M. R.; Martinho, J. M. G.; Xu, R.; Winnik, M. A. *Macromolecules* **1995**, *28*, 4750−4751. (b) Farinha, J. P. S.; d'Oliviera, J. M. R.; Martinho, J. M. G.; Xu, R.; Winnik, M. A. *Langmuir* **1998**, *14*, 2291−2296.

(20) Stejskal, J.; Koňák, Č.; Helmstedt, M.; Kratochvıl, P. *Collect. Czech. Chem. Commun.* **1993**, *58*, 2282−2289.

(21) Jada, A.; Hurtrez, G.; Siffert, B.; Riess, G. *Macromol. Chem. Phys.* **1996**, *197*, 3697−3710.

(22) *Molecular Dynamics in Restricted Geometries*; Klafter, J., Drake, J. M., Eds.; John Wiley & Sons: New York, 1989.

(23) (a) Morawetz, H. *Science* **1988**, *240*, 172−176. (b) Morawetz, H. *Collect. Czech. Chem. Commun.* **1993**, *58*, 2266−2271.

(24) Farinha, J. P. S.; Martinho, J. M. G.; Kawaguchi, S.; Yekta, A.; Winnik, M. A. *J. Phys. Chem.* **1996**, *100*, 12552−12558.

(25) Yekta, A.; Winnik, M. A.; Farinha, J. P. S.; Martinho, J. M. G. *J. Phys. Chem. A* **1997**, *101*, 1787−1792.

(26) Farinha, J. P. S.; Martinho, J. M. G. *J. Lumin.* **1997**, *72*, 914.

(27) Yekta, A.; Winnik, M. A. In *Solvents and Self-Organization of Polymers*; NATO ASI Series, Vol. 327; Webber, S. E., Munk, P., Tuzar, Z., Eds.; Kluwer Academic Publishers: Dordrecht, The Netherlands, 1996; pp 433−455.

(28) (a) Schillén, K.; Yekta, A.; Ni, S.; Winnik, M. A. *Macromolecules* **1998**, *31*, 210−212. (b) Schillén, K.; Yekta, A.; Ni, S.; Winnik, M. A. *Prog. Colloid Polym. Sci.*, in press.

(29) Farinha, J. P. S.; Schillen, K.; Winnik, M. A. *J. Phys. Chem. B* **1999**, *103*, 2487−2495.

(30) Duhamel, J.; Yekta, A.; Ni, S.; Khaykin, Y.; Winnik. M. A. *Macromolecules* **1993**, *26*, 6255−6260.

(31) Wang, Y.; Kausch, C. M.; Chun, M.; Quirk, R. P.; Mattice, W. L. *Macromolecules* **1995**, *28*, 904−911.

(32) Martin, T. J.; Webber, S. E. *Macromolecules* **1995**, *28*, 8845−8854.

(33) Liu, G. *Can. J. Chem.* **1995**, *37*, 1995−2003.

(34) Bednář , B.; Karásek, L.; Pokorný , J. *Polymer* **1996**, *27*, 5261−5268.

(35) Creutz, S.; van Stam, J.; Antoun, S.; De Schryver, F. C.; Jérôme, R. *Macromolecules* **1997**, *30*, 4078−4083.

(36) Liu, G.; Smith, C. K.; Hu, N.; Tao, J. *Macromolecules* **1996**, *29*, 220−227.

(37) Liu, G. *J. Phys. Chem.* **1995**, *99*, 5465−5470.

(38) Eckert, A. R.; Webber, S. E. *Macromolecules* **1996**, *29*, 560−567.

(39) (a) Ni, S.; Zhang, P.; Wang, Y.; Winnik. M. A. *Macromolecules* **1996**, *27*, 5742−5750. (b) Tcherkasskaya, O.; Ni, S.; Winnik, M. A. *Macromolecules* **1996**, *29*, 610−616. (c) Tcherkasskaya, O.; Spiro, J. G.; Ni, S.; Winnik, M. A. *J. Phys. Chem.* **1996**, *100*, 7114−7121. (d) Nakashima, K.; Duhamel, J.; Winnik, M. A. *J. Phys. Chem.* **1993**, *97*, 10702−10707. (e) Nakashima, K.; Liu, Y. Sh.; Zhang, P.; Duhamel, J.; Feng, J.; Winnik, M. A. *Langmuir* **1993**, *9*, 2825−2831.

(40) Katime, I.; Quintana, J. R.; Valenciano, R.; Strazielle, C. *Polymer* **1986**, *27*, 742−746.

(41) Berne, B. J.; Pecora, P. *Dynamic Light Scattering with Applications to Chemistry, Biology and Physics*, reprint ed.; Robert E. Krieger Publishing Co.: FL, 1990.

(42) Chu, B. *Laser Light Scattering: Basic Principles and Practice*, 2nd ed.; Academic Press: San Diego, 1991.

(43) Štěpánek, P. In *Dynamic Light Scattering: The Method and Some Applications*; Brown, W., Ed.; Oxford University Press: Oxford, U.K., 1993; pp 177−241.

(44) (a) Jakeš, J. *Czech. J. Phys.* **1988**, *B38*, 1305−1316. (b) Jakeš, J. *Collect. Czech. Chem. Commun.* **1995**, *60*, 1781−1797.

(45) Cogan, K. A.; Gast, A. P. *Macromolecules* **1990**, *23*, 745−753.

(46) Cummins, H. Z.; Pusey, P. N. In *Photon Correlation Spectroscopy and Velocimetry*; Cummins, H. Z.; Pike, E. R., Eds.; Plenum Press: New York, 1977; pp 164−186.

(47) Förster, Th. *Z. Naturforsch* **1949**, *4a*, 321.

(48) Berlmann, I. B. *Energy Transfer Parameters of Aromatic Compounds*; Academic Press: New York, 1973.

(49) Baumann, J.; Fayer, M. D. *J. Chem. Phys.* **1986**, *85*, 4087−4107.
(50) Blumen, A.; Klafter, J.; Zumofen, G. *J. Chem. Phys.* **1986**, *84*, 1397−1401, and references cited therein.
(51) Flory, P. J. *Principles of Polymer Chemistry*; Cornell University Press: Ithaca, NY, 1953.
(52) Hilfiker, R.; Chu, B.; Xu, Z. *J. Colloid Interface Sci.* **1989**, *133*, 176−184.
(53) Helfand, E.; Tagami, Y. *J. Chem. Phys.* **1972**, *56*, 3592−3601.
(54) Oranli, L.; Bahadur, P.; Riess, G.; *Can. J. Chem.* **1985**, *63*, 2691−2696.
(55) Rager, T.; Meyer, W. H.; Wegner, G.; Winnik, M. A. *Macromolecules* **1997**, *30*, 4911−4919.
(56) Douglas, J. F.; Roovers, J.; Freed, K. F. *Macromolecules* **1990**, *23*, 4168−4180.
(57) Yamakawa, H. *Modern Theory of Polymer Solutions*; Harper & Row: New York, 1971.
(58) Qin, A.; Tian, M.; Ramireddy, C.; Webber, S. E.; Munk, P.; Tuzar, Z. *Macromolecules* **1994**, *27*, 120−126.
(59) Burchard, W.; Schmidt, M.; Stockmayer, W. H. *Macromolecules* **1980**, *13*, 1265−1272.
(60) Antonietti, M.; Bremser, W.; Schmidt, M. *Macromolecules* **1990**, *23*, 3796−3805.
(61) (a) Mays, J. W.; Nan, S.; Lewis, M. E. *Macromolecules* **1991**, *24*, 4, 4857−4860. (b) Lewis, M. E.; Nan, S.; Yunan, W.; Li, J.; Mays, J. W.; Hadjichristidis, N. *Macromolecules* **1991**, *24*, 6686−6689.
(62) King, T. A.; Treadaway, M. F. *J. Chem. Soc., Faraday Trans. 2* **1977**, *73*, 1616−1626.
(63) Patterson, G. D. *Adv. Polym. Sci.* **1983**, *48*, 126−159.
(64) Yoshizaki, T.; Hayashi, H.; Yamakawa, H. *Macromolecules* **1994**, *27*, 4259−4262.
(65) Flory, P. J. *Statistical Mechanics of Chain Molecules*; Interscience Publishers: New York, 1969.
(66) Aharoni, S. M. *Macromolecules* **1983**, *16*, 1722−1728.
(67) *Handbook of Chemistry and Physics*, 75th ed.; Lide D. R., Ed.: CRC Press, Inc.: Boca Raton, FL, 1994; p 9-2.
(68) O'Reilly, J. M.; Teegarden, D. M.; Wignall, G. D. *Macromolecules* **1985**, *18*, 2747−2752.
(69) Yoon, D. Y.; Flory, P. J. *Macromolecules* **1976**, *9*, 299−303.
(70) *Encyclopedia of Polymer Science and Engineering*, Vol. 10; Mark, H. F., Bikales, N. M., Overberger, C. G., Menges, G., Eds.: John Wiley & Sons: New York, 1987; p 132.
(71) The weight-average radius of gyration is converted to a *z*-average using the relation (Kirste, R. G.; Kruse, W. A.; Ibel, K., D. Y. *Polymer* **1975**, *16*, 120−124.): $(R_g^z)^2 = (R_g^w)^2/(1 + U)/(1 + 2U)$, where the polydispersity factor, $U \equiv (M_w^{uni}/M_n^{uni}) - 1$.
(72) Isotactic PMMA (i-PMMA) has larger dimensions. Viscosity measurements suggest that i-PMMA chains are ca. 30% more extended than a-PMMA; see: Jenkins, R.; Porter, R. S. *Polymer* **1982**, *23*, 105−111.
(73) Brown, D. S.; Dawkins, J. V.; Farnell, A. S.; Taylor, G. *Eur. Polym. J.* **1987**, *23*, 463−467.
(74) Schillén K.; Classon, P. M.; Malmsten, M.; Linse, P.; Booth, C. *J. Phys. Chem. B* **1997**, *101*, 4238−4252, and references cited therein.